Available online at www.sciencedirect.com
SCIENCE DIRECT®
Biochemical Pharmacology 67 (2004) 77–85
Biochemical Pharmacology
www.elsevier.com/locate/biochempharm

Flavin-dependent antioxidant properties of a new series of *meso*-*N*,*N*′-dialkyl-imidazolium substituted manganese(III) porphyrins

Remy Kachadourian[a], Chris A. Johnson[b], Elysia Min[a], Ivan Spasojevic[c], Brian J. Day[a,d,e,*]

[a]*Department of Medicine, National Jewish Medical and Research Center, Denver, CO, USA*
[b]*Department of Pediatrics, National Jewish Medical and Research Center, Denver, CO, USA*
[c]*Department of Biochemistry, Duke University Medical Center, Durham, NC, USA*
[d]*Department of Medicine, University of Colorado Health Sciences Center, Denver, CO, USA*
[e]*Department of Pharmaceutical Sciences, University of Colorado Health Sciences Center, Denver, CO, USA*

Received 6 June 2003; accepted 21 August 2003

Abstract

A number of synthetic manganese complexes exhibit both *in vitro* and *in vivo* catalytic antioxidant activities. This study reports that the antioxidant potencies of a new series of *meso*-*N*,*N*′-dialkyl-imidazolium substituted manganese(III) porphyrins are dependent, in part, on their ability to redox cycle with endogenous flavin-dependent oxidoreductases. Inhibition of lipid peroxidation activities of these novel cationic porphyrins was compared using rat brain homogenate as a source of lipids and endogenous oxidoreductases. Iron and ascorbate was used as initiators of lipid peroxidation, and two indices of lipid peroxidation (thiobarbituric acid reactive species (TBARS) and F_2-isoprostanes) were determined. All *meso*-*N*,*N*′-dialkyl-imidazolium substituted porphyrins tested were potent inhibitors of lipid peroxidation with IC_{50} ranging from 0.1 to 34 μM with a metal-dependent potency of Mn(III) ⩾ Co(III) > Zn(II). A flavin-dependent oxidoreductase antioxidant process was supported by the ability of the diphenyleneiodonium chloride (DPI, a flavoenzyme inhibitor) to decrease the potency of Mn-porphyrins in the lipid peroxidation model and that Mn-porphyrins stimulate NADPH oxidation in rat brain homogenates. These data suggest that metalloporphyrins may have differential antioxidant effects in tissues due to the presence or absence of flavin-dependent oxidoreductases.

Keywords: Metalloporphyrins; Lipid peroxidation; TBARS; F_2-isoprostanes; Diphenyleneiodonium; Diaphorase

1. Introduction

Several classes of synthetic metal complexes are currently under investigation as SOD mimics, including manganese complexes of porphyrins, salen, and cyclic polyamines [1]. *In vitro*, metalloporphyrins exhibit other antioxidant capacities in addition to superoxide dismuting activity such as catalase-like activity [2], inhibition of lipid peroxidation [3] and scavenging of peroxynitrite [4–6]. In cell-culture models, they have been shown to protect neuronal cells from excitotoxic cell death [7], and to protect endothelial cells against paraquat-induced injury [8]. *In vivo*, they partially rescue a lethal phenotype in a manganese superoxide dismutase knock-out mouse [9], protect against reperfusion injuries [10] and inhibit autoimmune-induced diabetes [11].

Manganese(III) *meso*-tetrakis(*N*-methylpyridinium-2-yl)porphyrin (MnTM-2-PyP^{5+}) is a potent SOD mimic employing the Mn(III)/Mn(II) couple in the catalysis of O_2^- dismutation [12] and was 15-fold more potent antioxidant as CuZnSOD in a model of lipid peroxidation [3]. Substitution of *ortho*-*N*-methyl pyridinium with *N*-ethyl was found to decrease the interaction with DNA [12]

* Corresponding author. Tel.: +1-303-398-1121; fax: +1-303-270-2168.
E-mail address: DayB@NJC.ORG (B.J. Day).

Abbreviations: AEOL 10113 or MnTE-2-PyP^{5+}, manganese(III) *meso*-tetrakis(*N*-ethylpyridinium-2-yl)porphyrin; AEOL 10123 or MnTDM-1,3-IP^{5+}, manganese(III) *meso*-tetrakis(*N*,*N*′-dimethylimidazolium-2-yl)porphyrin; AEOL 10150 or MnTDE-1,3-IP^{5+}, manganese(III) *meso*-tetrakis(*N*,*N*′-diethylimidazolium-2-yl)porphyrin; AEOL 10158 or MnTDP-1,3-IP^{5+}, manganese(III) *meso*-tetrakis(*N*,*N*′-dipropylimidazolium-2-yl)-porphyrin; BHT, butylated hydroxytoluene; CoTDM-1,3-IP^{5+}, cobalt(III) *meso*-tetrakis(*N*,*N*′-dimethylimidazolium-2-yl)porphyrin; DPI, diphenyleneiodonium chloride; EDTA, ethylenediaminetetraacetic acid; EUK-8, manganese(III) salen; F_2-IP, F_2-isoprostanes; 2-HE, 2-hydroxyestradiol; ILP, inhibition of lipid peroxidation; 2-ME, 2-methoxyestradiol; MDA, malondialdehyde; MnTBAP, manganese(III) *meso*-tetrakis(4-carboxy-phenyl)porphyrin; NHE, normal hydrogen electrode; SOD, superoxide dismutase; TBARS, thiobarbituric acid reactive species; ZnTDM-1,3-IP^{5+}, zinc(II) *meso*-tetrakis(*N*,*N*′-dimethylimidazolium-2-yl)porphyrin.

0006-2952/$ – see front matter © 2003 Elsevier Inc. All rights reserved.
doi:10.1016/j.bcp.2003.08.036

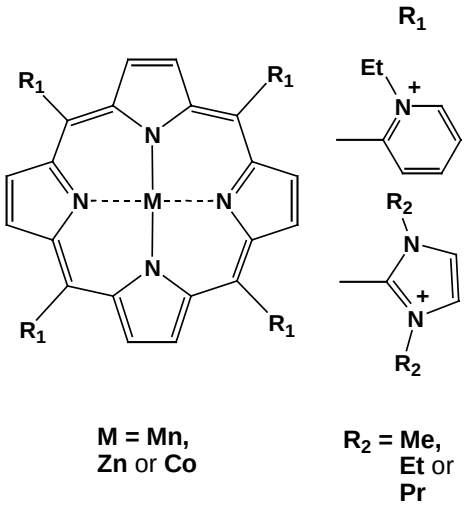

Fig. 1. Chemical structures of the metalloporphyrins analyzed, where the metal (M) is either manganese (Mn), cobalt (Co) or zinc (Zn) and R_1 is either an ethyl pyridinium [MnTE-2-PyP^{5+}], or an alkyl substituted imidazolium such as methyl (Me) [MnTDM-1,3-IP^{5+}, CoTDM-1,3-IP^{5+} and ZnTDM-1,3-IP^{4+}], or ethyl (Et) [MnTDE-1,3-IP^{5+}], or propyl (Pr) [MnTDP-1,3-IP^{5+}].

and to improve the pharmacodynamic properties. However, MnTM-2-PyP^{5+} and its *N*-ethyl analog MnTE-2-PyP^{5+} [12] are mixtures of four atropisomers [13,14], making them difficult to develop as pharmaceuticals.

In the search of new potent SOD mimics that do not exist as atropisomers, a new series of analogs carrying four *N*,*N*′-dialkylimidazoliums in *meso* positions have been prepared [US Patent #6,544,975B1]: MnTDM-1,3-IP^{5+}, and its *N*,*N*′-diethyl and *N*,*N*′-di-*n*-propyl analogs, MnTDE-1,3-IP^{5+} and MnTDP-1,3-IP^{5+} (Fig. 1). Their antioxidant capacity was determined in a lipid peroxidation model and was measured in terms of both the formation of TBARS [3] and F_2-isoprostanes [15]. The zinc and cobalt complexes of H_2TDM-1,3-IP^{4+} were prepared as controls. Mechanistic studies, to confirm the redox cycling of the compounds with flavin-containing enzymes, were done with rat brain homogenates by measuring the stimulation of NADPH consumption by *meso*-*N*,*N*′-dialkyl-imidazolium substituted porphyrins. These studies found that *meso*-*N*,*N*′-dialkyl-imidazolium substituted porphyrins were potent inhibitors of lipid peroxidation and this activity was dependent in part on their ability to redox cycle with flavin-containing enzymes.

2. Materials and methods

2.1. Metal complexes

The synthesis of *meso*-tetrakis(*N*,*N*′-dimethylimidazolium-2-yl)porphyrin (H_2TDM-1,3-IP^{5+}) was previously described [16], and the MnTDM-1,3-IP^{5+}, and its *N*,*N*′-ethyl and *N*,*N*′-di-*n*-propyl analogs, MnTDE-1,3-IP^{5+} and MnTDP-1,3-IP^{5+}, were prepared as previously described in US Patent #6,544,975B1 and were a kind gift from Incara Pharmaceuticals. The three compounds showed the same molar absorptivity at 466 nm, $\log \varepsilon = 5.09$. MnTE-2-PyP^{5+} was prepared as described previously [12,17]. The zinc and cobalt complexes of *meso*-tetrakis(*N*,*N*′-dimethylimidazolium-2-yl)porphyrin, ZnTDM-1,3-IP^{4+} (UV-Vis in H_2O, $\log \varepsilon_{418\,nm} = 4.95$) and CoTDM-1,3-$IP^{5+}$ (UV-Vis in H_2O, $\log \varepsilon_{418\,nm} = 4.78$) were also prepared as described previously [17], using *meso*-tetrakis(*N*,*N*′-dimethylimidazole-2-yl)porphyrin (Mid-Century Chemicals), methyl *p*-toluene-sulfonate (Aldrich), and $ZnCl_2$ (Aldrich) and $CoCl_2$ (Sigma), respectively. The complexes contained Zn^{2+}, Mn^{3+} or Co^{3+}, as demonstrated by the hypsochromic shift of the Soret band upon the reduction of the metal center by ascorbic acid in the case of the Mn^{3+} or Co^{3+} complexes (20- and 12-nm, respectively). Purity of the metal complexes was assessed by HPLC analysis as previously described [13] and was found to be greater than 97%. The EUK-8 was a kind gift from Calbiochem.

2.2. Other chemicals

L-Ascorbic acid, cytochrome *c*, xanthine, *n*-butanol, BHT, iron(II) chloride, phosphoric acid (85%), sodium hydroxide, potassium phosphate, EDTA, 1,1,3,3-tetramethoxypropane, bis-trimethylsilyl trifluoroacetamide, estradiol, 2-methoxyestradiol, 2-hydroxyestradiol, DPI and β-nicotinamide adenine dinucleotide phosphate reduced form tetrasodium salt (NADPH) were purchased from Sigma. Acetone, concentrated hydrochloric acid, 4,6-dihydroxy-2-mercaptopyrimidine (thiobarbituric acid), pentafluorobenzyl bromide, *N*,*N*′-diisopropylethylamine and Trolox were purchased from Aldrich. Manganese(II) chloride, methanol and acetonitrile (HPLC grade) were purchased from Fisher and ethanol USP from AAPER Alcohol and Chemical Co. Prostaglandin $F_2\alpha$-d_4 (d_4-$PGF_2\alpha$) and 8-iso prostaglandin $F_2\alpha$-d_4 (d_4-8epi-$PGF_2\alpha$) were purchased from Cayman Chemical. Xanthine oxidase was from Roche Diagnostics Corp. All aqueous solutions were prepared using Milli-Q Plus PF water.

2.3. Electrochemistry

The metal-centered redox potentials were established as described previously, using a Voltammetric Analyzer model 600 (CH Instrument) and a 3-electrode setup system in a small volume cell (0.5 mL), consisting of a 3-mm in diameter button glassy carbon working electrode (Bioanalytical Systems), a standard Ag/AgCl reference electrode, and a 0.5-mm platinum wire as an auxiliary electrode [12]. The samples were analyzed as solutions containing 0.5 mM metalloporphyrin and 0.1 M NaCl in a 0.05 M phosphate buffer (pH 7.8). Scan rates were 10–500 mV/s, typically 100 mV/s, and the potentials were

standardized against potassium ferricyanide/potassium ferrocyanide couple.

2.4. Superoxide dismutase activity

The SOD-like activities were measured using the xanthine/xanthine oxidase system as a source of superoxide and ferricytochrome *c* as its indicating scavenger [18]. Superoxide was produced at the rate of 1.2 μM/min, and reduction of ferricytochrome *c* was followed at 550 nm. Assays were conducted in the presence of 0.1 mM EDTA in 0.05 M phosphate buffer (pH 7.8), at 25°. The metalloporphyrins analyzed do not interfere with the activity of xanthine oxidase, as checked by following urate accumulation at 295 nm in the absence of cytochrome *c*, nor did they interfere by reoxidizing cytochrome *c*.

2.5. Catalase activity

Catalase-like activity was measured as described previously, using a Clark-type electrode to monitor the release of oxygen [19]. The reaction chamber volume was 1 mL and the electrode was calibrated with an air-equilibrated 50 mM phosphate buffer at 25° (0.24 mM of oxygen) and zeroed by consuming the dissolved oxygen by addition of excess sodium dithionite. Reactions were carried out in a 50 mM phosphate buffer, pH 7.8, containing 0.1 mM EDTA. H_2O_2 solutions were prepared by diluting a 30% (v/v) stock solution with ultrapure water. H_2O_2 concentrations were verified spectrophotometrically using $\varepsilon_{240\,nm} = 44\ M^{-1}\ cm^{-1}$ [20]. Reactions were performed with 1 mM H_2O_2 and varying concentrations of metalloporphyrins (5–50 μM). The rate of oxygen released was converted to the rate of H_2O_2 consumed by multiplying by a factor of two, which assumes that two molecules of H_2O_2 are consumed for each O_2 produced [$2H_2O_2 \rightarrow O_2 + H_2O$]. The rates of H_2O_2 consumption were plotted against metalloporphyrins concentrations and the slope was used to obtain the pseudo first-order rate constants.

2.6. Preparation of rat brain homogenates

Frozen adult Sprague–Dawley rat brains (Pel-Freez) were homogenized with a polytron (Turrax T25) in 5 volumes of ice-cold 50 mM potassium phosphate at pH 7.4. Homogenate protein concentration was determined with the Coomassie Plus protein assay (Pierce) using bovine serum albumin as a standard. The homogenate volume was adjusted with buffer to give a final protein concentration of 10 mg/mL and frozen as aliquots at −80°.

2.7. Oxidation of rat brain homogenates

Rat brain homogenates (0.2 mg/mL of protein concentration) were incubated with varying concentrations of antioxidant at 37° for 15 min. When used, DPI was added from a 10 mM stock DMSO solution. Oxidation of the rat brain homogenate was initiated by the addition of 0.1 mL of a freshly prepared anaerobic stock solution containing iron(II) chloride (0.25 mM) and ascorbate (1 mM) as previously reported by Braughler *et al.* [21]. Samples (final volume 1 mL) were placed in a shaking water bath at 37° for 30 min. The reactions were stopped by the addition of 0.1 mL of a stock butylated hydroxytoluene (60 mM) solution in ethanol.

2.8. TBARS measurement

The concentration of TBARS in rat brain homogenates was used as an index of lipid peroxidation [22]. MDA standards were obtained by adding 8.2 μL of 1,1,3,3-tetramethoxypropane in 10 mL of 0.01 M HCl and mixing for 10 min at room temperature. This stock was further diluted in water to give standards that ranged from 0.25 to 25 μM. Samples or standards (200 μL) were acidified with 200 μL of 0.2 M phosphoric acid in 1.5 mL locking microfuge tubes. The color reaction was initiated by the addition of 25 μL of a 0.11 M thiobarbituric acid solution and samples were placed in a 90° heating block for 45 min. TBARS were extracted with 0.5 mL of *n*-butanol by vortexing samples for 3 min and chilling on ice for 1 min. The samples were then centrifuged at 12,000 *g* for 3 min, 150 μL aliquots of the *n*-butanol phase were placed in each well of a 96-well plate and read at 535 nm in a plate-reader (Spectramax 340PC, Molecular Devices) at 25°. Sample absorbances were converted to MDA equivalencies (μM) by extrapolation from the MDA standard curve. None of the antioxidants at concentrations employed in these studies affected the reaction of MDA standards with thiobarbituric acid and reactions without TBA were used as subtraction blanks.

2.9. F_2-isoprostanes measurement

F_2-isoprostanes were isolated from treated samples of rat brain homogenate and measured by GC/MS using electron capture negative ionization following derivatization as described previously [23], with modifications. Lipids samples (0.8 mL) were extracted using 2 mL of a mixture methanol/chloroform (1:1) (modified Bligh and Dyer extraction). Stable isotope internal standards, d_4-$PGF_2\alpha$ and d_4-8epi-$PGF_2\alpha$ were added. After drying the organic phase under nitrogen, samples were saponified using 0.5 mL of methanol and 0.5 mL of 1 M NaOH, and left at room temperature for 1 hr. The pH was then lowered to 2 using 0.5 mL of 1 M HCl, samples washed twice with 1 mL of iso-octane, and extracted twice with 1 mL ethyl acetate. Extracts were washed once with 1 mL distilled water and the solvent evaporated under nitrogen. Samples were then treated by adding 25 μL of 1% pentafluorobenzyl bromide in acetonitrile and 25 μL of 1% *N*,*N*′-diisopropylethylamine in acetonitrile. Reaction mixtures were

vortexed, left at room temperature for 20 min, and the solvent evaporated under nitrogen. The trimethylsilyl ether derivatives were formed by adding 20 μL of bis-trimethylsilyl trifluoroacetamide and 20 μL of acetonitrile, and reacting for 15 min at 60°. Samples were then analyzed on a Trace GC/MS (Thermo Finnigan) operated in the negative ion chemical ionization mode with methane as the carrier gas. The column was a ZB-1 (15 m × 2.5 mm i.d.) with a 0.25 mm film thickness (Phenomenex) temperature programmed from 150 to 300° at 15° min^{-1}.

2.10. NADPH oxidase assay

Rat brain homogenate-dependent NADPH oxidation to $NADP^+$ was followed spectrophotometrically (UV2401 PC, Shimadzu) at 340 nm. Reactions were performed in 1 mL of buffer containing 0.1 M potassium phosphate (pH 7.8), 1 mg/mL brain homogenate protein and 250 μM NADPH. Reactions were followed for 1 min at 25°. The change in absorbance/minute was converted to nmol NADPH consumed/minute using NADPH's extinction coefficient ($\varepsilon = 6.187 \times 10^2$ L/mol mm). Reactions were performed in triplicate.

2.11. Statistical analysis

Data were presented as their means ± SE. The inhibitory concentration of antioxidants that decreased the degree of lipid peroxidation by 50% (IC_{50}) were determined by fitting a sigmoidal curve with variable slope to the data (GraphPad Prizm). Statistical significance between IC_{50}s were determined by *F*-test (GraphPad Prizm). Statistical significance between groups was determined using a one-way ANOVA with a Tukey's range test where significance was set at a *P*-value <0.05 (GraphPad Prizm).

3. Results

3.1. Metal-centered redox potentials

The metal-centered redox potentials of MnTDM-1,3-IP^{5+}, MnTDE-1,3-IP^{5+}, MnTDP-1,3-IP^{5+} and CoTDM-1,3-IP^{5+} are given in Table 1. The three manganese(III) porphyrins exhibit near-reversible Mn(III)/Mn(II) electrochemistry on a glassy carbon electrode and similar metal-centered redox potentials. The values are 82–118 mV more positive then their corresponding *meso*-pyridinium analogs [12,17]. A slightly higher peak-to-peak separation than 59 mV (expected for a one electron transfer voltammetry) is commonly observed for manganese complexes with positively charged porphyrins. The cobalt complex, CoTDM-1,3-IP^{5+}, however, exhibits a very large peak-to-peak separation (422 mV), indicating a slow electron transfer, thus making the half-wave potential (+277 mV vs. NHE) an unreliable approximation of the standard redox potential.

3.2. SOD activity

The imidazolium-substituted metalloporphyrins exhibited enhanced SOD-like activity in the indirect cytochrome *c* SOD assay as shown for MnTDM-1,3-IP^{5+} using an Asada plot (Fig. 2). SOD-like activities for the imidazolium-substituted metalloporphyrins are reported in Table 1 as the concentrations that inhibit 50% of the reduction of

Table 1
Comparisons of metalloporphyrins and other antioxidants

Compound	$E_{1/2}$ (mV vs. NHE)	SOD ($IC_{50}/10^{-8}$ M)[a]	$k(H_2O_2)$ (min^{-1})[b]	Antioxidant (IC_{50} μM)[c]	
				TBARS	F_2-IP
MnTE-2-PyP^{5+}	+228[d]	4.5[d]	2.0	0.1	0.1
MnTDM-1,3-IP^{5+}	+320	2.0	2.1	0.1	0.1
MnTDE-1,3-IP^{5+}	+346	1.8	2.2	0.1	0.1
MnTDP-1,3-IP^{5+}	+320	2.0	2.0	0.1	0.1
CoTDM-1,3-IP^{5+}	+277	167	n.a.	4.3	n.d.
ZnTDM-1,3-IP^{4+}	–	n.a.	n.a.	31.0	n.d.
EUK-8	−130[e]	120	2.0	0.1	n.d.
Trolox	–	–	–	15.0	n.d.
2-HE	–	–	–	0.3[f]	0.3
2-ME	–	–	–	1.3[f]	1.3
β-Estradiol	–	–	–	5.8[f]	6.8

n.a.: not active; n.d.: not determined.
[a] The margin error for SOD-like activities is ±10%.
[b] The margin error for catalase-like activities is ±20%.
[c] The antioxidant activity values are reported using a rat brain homogenate with a protein concentration ($c = 0.2$ mg/mL), except for the estrogens ($c = 0.4$ mg/mL).
[d] [27].
[e] [33].
[f] [25].

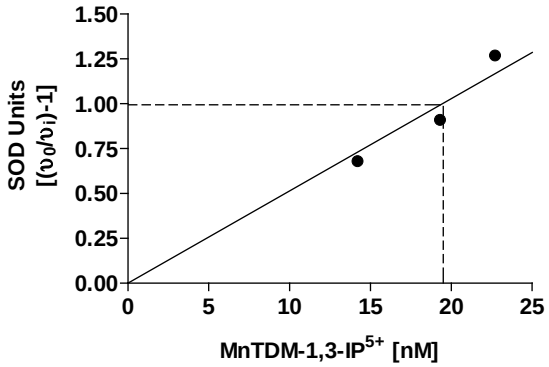

Fig. 2. Determination of the superoxide dismutase (SOD)-like activity of MnTDM-1,3-IP^{5+}. The IC_{50} is the concentration of compound that inhibits 50% of the reduction of cytochrome *c* by O_2^- generated by the xanthine/xanthine oxidase system, where v_0 is the rate of reduction of cytochrome *c* without compound and v_i is the rate of reduction in presence of the compound. The Asada plot of $[(v_0/v_i) - 1]$ vs. compound concentration is commonly used to define a unit of SOD activity.

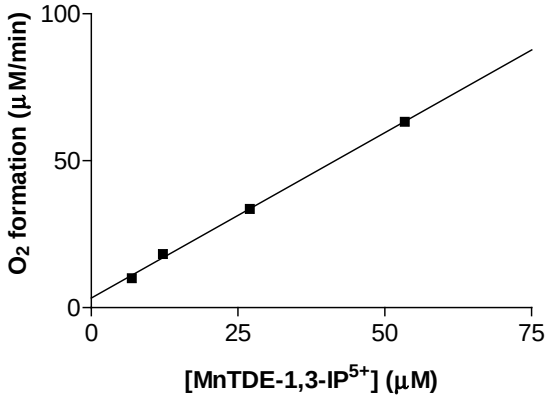

Fig. 3. Determination of the catalase-like activity of MnTDE-1,3-IP^{5+}. The dismutation of hydrogen peroxide forms molecular oxygen and water. The formation of oxygen is measured using a Clark electrode after mixing 1 mM of hydrogen peroxide with different amounts of the manganese complex (5–50 μM), and the pseudo-first rate constant of formation of oxygen being half of the pseudo-first rate constant of the consumption of hydrogen peroxide.

cytochrome *c* by superoxide (1 unit of SOD activity). SOD-like activities of MnTDM-1,3-IP^{5+}, MnTDE-1,3-IP^{5+}, MnTDP-1,3-IP^{5+} are similar (IC_{50}, 18–20 nM), over 2-fold higher than their corresponding *N*-alkylpyridinium analogs [13,15,31], and equal to the β-dichlorinated analog of MnTE-2-PyP^{5+} [17]. The SOD-like activity of the cobalt(III) complex is two orders of magnitude lower (IC_{50}, 1.67 μM), probably due to a slow electron transfer as indicated by the large peak-to-peak separation in the cyclic voltammetry experiment. As expected, the redox inactive analog ZnTDM-1,3-IP^{4+} had no measurable SOD-like activity.

3.3. Catalase-like activity

As shown previously for MnTBAP and MnTM-4-PyP^{5+} [2], the imidazolium-substituted metalloporphyrins can also undergo two-electron transfer to dismute hydrogen peroxide to form oxygen and water. The catalase-like activities of Mn-porphyrins were established by measuring oxygen formation in presence of excess hydrogen peroxide (1 mM) as illustrated by MnTDE-1,3-IP^{5+} (Fig. 3). The catalase activities for MnTE-2-PyP^{5+}, MnTDM-1,3-IP^{5+}, MnTDE-1,3-IP^{5+} and MnTDP-1,3-IP^{5+}, and are shown in Table 1. All four manganese(III) porphyrins exhibit similar pseudo first-order rate constants ($k \sim 2.0\ \text{min}^{-1}$), similar as well as to the manganese(III) salen complex EUK-8 whereas CoTDM-1,3-IP^{5+} and ZnTDM-1,3-IP^{4+} had no catalase-like activity.

3.4. Inhibition of lipid peroxidation

A method that has been widely used as an index of lipid peroxidation is the measurement of the TBARS [3]. This method has been criticized because of its lack of specificity when used for biological samples. A more recent method measures the formation of F_2-isoprostanes, a family of products that mainly result from the non-enzymatic oxidation of arachidonic acid [15]. This method, however, requires more processing steps, as well as access to GC/MS or LC/MS. The measurement of TBARS and F_2-isoprostanes were compared from the same iron/ascorbate-induced oxidation of a rat brain homogenate with and without antioxidants. Animal tissue homogenate was used as source of lipids since it was previously shown that the peroxidase activity of metalloporphyrins depends on the presence of reductants [24].

All *meso-N,N′*-dialkyl-imidazolium substituted porphyrins tested were potent inhibitors of lipid peroxidation with a metal-dependent potency of Mn(III) ⩾ Co(III) > Zn(II) wherein the manganese-containing imidazolium-substituted porphyrins were two orders of magnitude more potent than the water soluble Vitamin E analog Trolox (Fig. 4). The antioxidant activities for MnTDM-1,3-IP^{5+}, MnTDE-1,3-IP^{5+} and MnTDP-1,3-IP^{5+} are given in Table 1

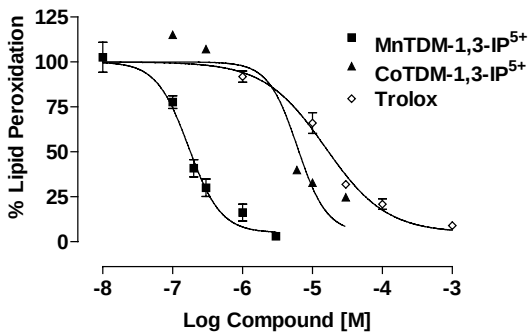

Fig. 4. Comparison of manganese and cobalt complexes of H_2TDM-1, 3-IP^{4+} to Trolox in their ability to inhibit iron/ascorbate mediated oxidation of rat brain homogenate using the TBARS assay. The ligation of a manganese metal significantly enhanced the porphyrin's ability to inhibit lipid peroxidation compared to cobalt.

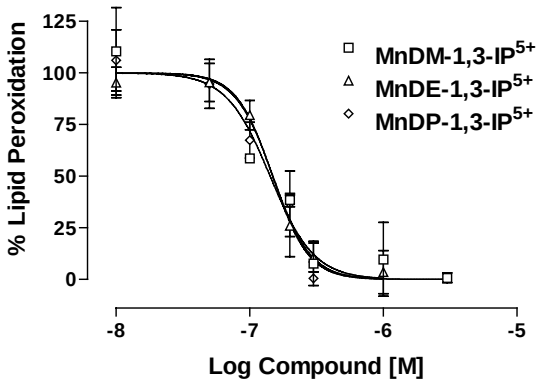

Fig. 5. Ability of Mn-porphrins to inhibit iron/ascorbate mediated oxidation of rat brain homogenate by quantification of F_2-isoprostanes using GC/MS after extraction and derivatization. All of the imidazolium substituted manganese porphyrins inhibited F_2-isoprostane formation with IC_{50}s that were not statistically different, $P > 0.05$.

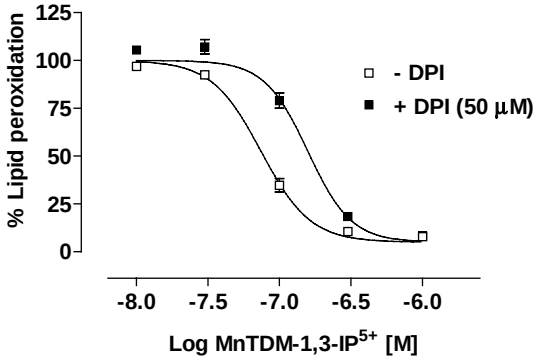

Fig. 6. Effect of inhibiting flavin-containing enzymes with DPI (50 μM) on the antioxidant activity of MnTDM-1,3-IP^{5+} in an iron/ascorbate-mediated oxidation of rat brain homogenate using the TBARS assay. The IC_{50} for the −DPI curve was 74 nM vs. 158 nM IC_{50} for the +DPI curve. The IC_{50}s were significantly different, $P = 0.0001$.

as their IC_{50}s (concentration that inhibits 50% of lipid peroxidation). The manganese(III) salen complex EUK-8 exhibits similar activity as the manganese(III) porphyrins tested, an activity that is unexpectedly high compared to EUK-8's relatively low SOD activity (Table 1). As expected from their low or absent SOD activities, CoTDM-1,3-IP^{5+} and ZnTDM-1,3-IP^{4+} were not potent inhibitors of lipid peroxidation.

Due to the ambiguous nature of the TBAR assay, the compounds were also assessed for their ability to inhibit lipid peroxidation by measuring the formation of F_2-isoprostanes (Fig. 5). This study shows that the IC_{50}s of the catalytic antioxidants described above using both the TBARS assay and the measurements of F_2-isoprostanes are the same within the margin of errors (Table 1). This is also true for several stochiometric antioxidants that exhibit different redox active structures such as β-estradiol, 2-methoxyestradiol and 2-hydroxyestradiol [25].

3.5. Flavin-dependence of Mn-porphyrin antioxidant activity

To assess the possible role of flavin-containing proteins in the antioxidant properties of Mn-porphyrin, the potency of MnTDM-1,3-IP^{5+} in the lipid peroxidation model was determined in the presence or absence of DPI, an inhibitor of flavin-containing oxidioreductases [26]. Inhibition of flavin-containing oxidoreductases by DPI in the rat brain homogenate shifted the MnTDM-1,3-IP^{5+} dose–response curve to the right by doubling the IC_{50} (74 nM without DPI compared to 174 nM with DPI) indicating a loss of potency (Fig. 6). MnTDM-1,3-IP^{5+} was assessed for diaphorase activity by measuring its ability to stimulate NADPH oxidation and further verify that these compounds could redox cycle with flavin-containing proteins in the rat brain homogenates. The addition of MnTDM-1,3-IP^{5+} to rat brain homogenates stimulated NADPH oxidation by 3-fold and this activity was inhibited by the presence of DPI

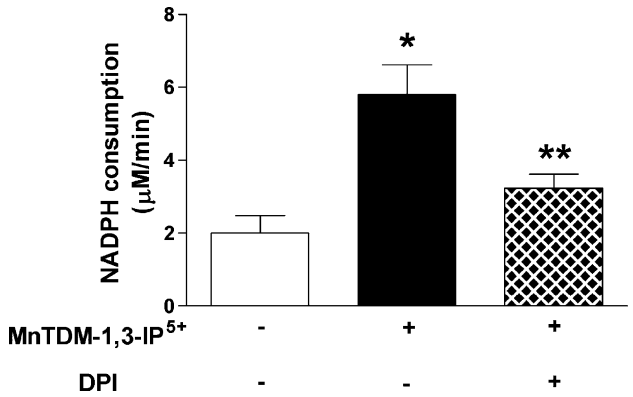

Fig. 7. The stimulation of NADPH consumption by MnTDM-1,3-IP^{5+} on rat brain homogenate. The NADPH consumption induced by the presence MnTDM-1,3-IP^{5+} (10 μM) is inhibited by DPI (100 μM). The direct reaction rate of the Mn-porphyrin with NADPH was less than the control, which consisted of the rat brain homogenate and NADPH. $^{*}P = 0.01$ vs. open bar and $^{**}P = 0.05$ vs. hatched bar.

(Fig. 7). Similar results were found with the other imidazolium-substituted porphyrin as well as the pyridinium-substituted porphyrins (data not shown). The ability of the DPI to shift the potency of Mn-porphyrins in the lipid peroxidation model and the fact that they stimulate NADPH oxidation in rat brain homogenates supports the concept that a flavin-dependent oxidoreductase process drives a portion of their antioxidant activity.

4. Discussion

Previous work has focused on the development and activities of *meso*-substituted pyridinium manganese porphyrins which have fast *in vitro* rate constants for the dismutation of superoxide [12,17] and are potent inhibitors of lipid peroxidation [3]. When compared to their *meso*-pyridinium analogs, the new generation of *meso*-imidazolium derivatives exhibit both higher metal-centered redox

potentials and SOD activities, thus confirming the correlation between these two properties [27]. In terms of antioxidant properties *in vitro*, MnTDM-1,3-IP^{5+}, MnTDE-1,3-IP^{5+} and MnTDP-1,3-IP^{5+} do not exhibit significant differences from their *meso*-pyridinium substituted analogues. Yet, some differences may be observed *in vivo*, due to differences in pharmacokinetics and toxicity. For instance, although MnTE-2-PyP^{5+} and MnTDE-1,3-IP^{5+} exhibit comparable efficacies *in vitro*, they have shown significant differences in their therapeutic indexes *in vivo* [28]. There are also differences in their retention on a C18 column that may reflect changes in cellular distributions and half-lives [13].

Hydrogen peroxide has been proposed to be a potent cell-signaling agent involved in cell differentiation and proliferation [29,30]. It can readily deplete cells of glutathione and thus change the redox potential in the cell [31], thereby indirectly affecting cell signaling controlling proliferation and differentiation [32]. The catalase-like activity of manganese(III) salen complexes is thought to play a role in their protective effect in a rat stroke model [33]. Manganese(III) porphyrins also can scavenge hydrogen peroxide *in vitro* and protect cultured cells against its cytotoxic effects [2,34]. It has also been suggested that the ability of MnTE-2-PyP^{5+} to inhibit adoptive transfer of autoimmune diabetes may be due to its catalase-like activity [11], but this hypothesis remains to be tested. In general, the relevance of the catalase-like activities of metal complexes *in vivo* remains unclear, since the activity of these complexes pales in comparison to that of cellular catalase and glutathione peroxidases.

A correlation between SOD activity and inhibition of lipid peroxidation has been established for manganese(III) porphyrins [3], yet the differences of SOD-like activities between *meso*-pyridinium and *meso*-imidazolium derivatives appears too small to show a significant difference in this model. Interestingly, EUK-8, which has a much lower SOD activity, exhibits the same ability to inhibit lipid peroxidation as the manganese(III) porphyrins analyzed here. A similar effect has been observed with an uncharged manganese(III) glycolate porphyrin (AEOL 11201), which was effective in ameliorating injury in a rat colitis model and a potent antioxidant in the lipid peroxidation model [35]. Clearly, other factors besides redox potential and SOD activity are involved in determining a compound's efficacy in preventing lipid peroxidation, including hydrophobicity and their ability to chain-break the propagation of lipid peroxidation reactions.

F_2-isprostanes have emerged as popular index of lipid peroxidation [15]. Unlike other arachidonic acid enzymatic oxidation products, prostaglandins and leukotrienes, the F_2-isoprostanes are predominantly formed by the non-enzymatic oxidation by reactive oxygen species. Moreover, the F_2-isoprostanes are formed *in vivo* and possess biological activities similar to prostaglandins and may be responsible for some of the pro-inflammatory effects of oxidative stress [36,37]. An interesting observation was made when comparing the IC_{50}s of a wide range of structurally different antioxidants, in that all of them had similar values regardless whether TBARS or F_2-isoprostanes were used as the index of lipid peroxidation. This study confirms the utility of the TBARS assay in measuring the relative ability of antioxidants to inhibit lipid peroxidation *in vitro*, and remains a reliable screening method.

A number of redox active compounds can be readily reduced by cellular diaphorases, which are generally flavin-containing enzymes that have oxidoreductase functions and utilize either NADPH or NADH as a source of electrons [38]. Typically when compounds redox cycle with these cellular diaphorases, they have the potential to generate reactive oxygen species, as is the case for paraquat [39], doxirubicin [40], and ubiquinone [41]. Metal complexes, such as the Mn-porphyrins, are unique for they not only make reactive oxygen species, but can also consume them. Earlier studies have demonstrated the importance of cellular reductants, such as ascorbate and urate, in preserving the antioxidant function of Mn-porphyrins [24]. The current studies demonstrate that Mn-porphyrins can also use flavin-containing enzymes to enhance their antioxidant potencies in a lipid peroxidation model. Two pieces of data support this hypothesis and include the shift to the right of the dose response curve by a flavin protein inhibitor, DPI, and the ability of cationic Mn-porphyrins to stimulate NADPH consumption in the rat brain homogenate. These findings add yet another possible mechanism by which Mn-porphyrins could produce their antioxidant effects in biological systems.

The antioxidant effects of metalloporphyrins have always been considered to occur by the direct scavenging of oxidants. A number of possible implications arise when one considers that metalloporphyrins can redox cycle with cellular diaphorases. Many of the known cellular diaphorases are oxidoreductases that can either directly or indirectly generate reactive oxygen and/or nitrogen species and include nitric oxide synthases, NADPH oxidase, and cytochrome P450 reductase. It is worth noting that by inhibiting these enzymes, one could achieve a decrease in reactive oxygen and/or nitrogen species formation without directly scavenging them. In fact, some evidence for this exists in the literature where manganese(III) *meso*-tetrakis(*N*-methylpyridinium-4-yl)porphyrin has been shown to inhibit the production of NO from NOS [42]. The previously reported observations that iron and manganese containing porphyrins have been shown to inhibit the formation of nitrotyrosine in cell culture and animal models of inflammation [43–49] could also be explained by inhibition of either superoxide or nitric oxide formation rather than their direct reaction with peroxynitrite. The reaction of Mn-porphyrins with cellular diaphorases may also raise potential toxicity issues. Many of these cellular diaphorases perform critical functions in biological systems that may be disrupted by redox cycling with

Mn-porphyrins. In addition, the redox cycling of Mn-porphyrins with diaphorases may deplete cellular levels of NADPH and indirectly disrupt biosynthetic pathways. Another concern involves the possible net production of reactive oxygen species from Mn(II)-porphyrins reacting with molecular oxygen. This may be of particular concern under conditions of elevated oxygen tensions. Studies are currently underway to better characterize the reactions between known cellular diaphorases and Mn-porphyrins to better answer some of these issues.

In summary, the *meso*-*N*,*N*′-dialkyl-imidazolium substituted porphyrins tested were potent inhibitors of lipid peroxidation with IC_{50} ranging from 0.1 to 34 μM and with a metal-dependent potency of $Mn(III) \gg Co(III) > Zn(II)$. The ability of the DPI, a flavoenzyme inhibitor, to shift the potency of Mn-porphyrins in the lipid peroxidation model and that Mn-porphyrins stimulate NADPH oxidation in rat brain homogenates supports a partial flavin-dependent oxidoreductase process. These data suggest that these Mn-porphyrins may have different antioxidant potencies in tissues due to the presence or absence of flavin-dependent oxidoreductases.

Acknowledgments

The authors thank Drs. Robert Murphy, Ines Batinic-Haberle, James Crapo, and Irwin Fridovich for their helpful suggestions. This work was supported in part by NIH grants HL31992 and HL59602, and a grant from Incara Pharmaceuticals.

References

[1] Riley DP. Functional mimics of superoxide dismutase enzymes as therapeutic agents. Chem Rev 1999;99(9):2573–88.
[2] Day BJ, Fridovich I, Crapo JD. Manganic porphyrins possess catalase activity and protect endothelial cells against hydrogen peroxide-mediated injury. Arch Biochem Biophys 1997;347(2):256–62.
[3] Day BJ, Batinic-Haberle I, Crapo JD. Metalloporphyrins are potent inhibitors of lipid peroxidation. Free Radic Biol Med 1999;26(5/6):730–6.
[4] Szabo C, Day BJ, Salzman AL. Evaluation of the relative contribution of nitric oxide and peroxynitrite to the suppression of mitochondrial respiration in immunostimulated macrophages using a manganese mesoporphyrin superoxide dismutase mimetic and peroxynitrite scavenger. FEBS Lett 1996;381(1-2):82–6.
[5] Hunt JA, Lee J, Groves JT. Amphiphilic peroxynitrite decomposition catalysts in liposomal assemblies. Chem Biol 1997;4(11):845–58.
[6] Ferrer-Sueta G, Batinic-Haberle I, Spasojevic I, Fridovich I, Radi R. Catalytic scavenging of peroxynitrite by isomeric Mn(III) *N*-methylpyridylporphyrins in the presence of reductants. Chem Res Toxicol 1999;12(5):442–9.
[7] Patel M, Day BJ, Crapo JD, Fridovich I, McNamara JO. Requirement for superoxide in excitotoxic cell death. Neuron 1996;16(2):345–55.
[8] Day BJ, Shawen S, Liochev SI, Crapo JD. A metalloporphyrin superoxide dismutase mimetic protects against paraquat-induced endothelial cell injury, *in vitro*. J Pharmacol Exp Ther 1995;275(3):1227–32.
[9] Melov S, Schneider JA, Day BJ, Hinerfeld D, Coskun P, Mirra SS, Crapo JD, Wallace DC. A novel neurological phenotype in mice lacking mitochondrial manganese superoxide dismutase. Nat Genet 1998;18(2):159–63.
[10] Mackensen GB, Patel M, Sheng H, Calvi CL, Batinic-Haberle I, Day BJ, Liang LP, Fridovich I, Crapo JD, Pearlstein RD, Warner DS. Neuroprotection from delayed postischemic administration of a metalloporphyrin catalytic antioxidant. J Neurosci 2001;21(13):4582–92.
[11] Piganelli JD, Flores SC, Cruz C, Koepp J, Batinic-Haberle I, Crapo J, Day B, Kachadourian R, Young R, Bradley B, Haskins K. A metalloporphyrin-based superoxide dismutase mimic inhibits adoptive transfer of autoimmune diabetes by a diabetogenic T-cell clone. Diabetes 2002;51(2):347–55.
[12] Batinic-Haberle I, Benov L, Spasojevic I, Fridovich I. The *ortho* effect makes manganese(III) *meso*-tetrakis(*N*-methylpyridinium-2-yl)porphyrin a powerful and potentially useful superoxide dismutase mimic. J Biol Chem 1998;273(38):24521–8.
[13] Kachadourian R, Menzeleev R, Agha B, Bocckino SB, Day BJ. High-performance liquid chromatography with spectrophotometric and electrochemical detection of a series of manganese(III) cationic porphyrins. J Chromatogr B: Anal Technol Biomed Life Sci 2002;767(1):61–7.
[14] Spasojevic I, Menzeleev R, White PS, Fridovich I. Rotational isomers of *N*-alkylpyridylporphyrins, and their metal complexes. HPLC separation, (1)H NMR and X-ray structural characterization, electrochemistry, and catalysis of $O_2^{\bullet -}$ disproportionation. Inorg Chem 2002;41(22):5874–81.
[15] Roberts LJ, Morrow JD. Measurement of F(2)-isoprostanes as an index of oxidative stress *in vivo*. Free Radic Biol Med 2000;28(4):505–13.
[16] Tjahjono DH, Akutsu T, Yoshioka N, Inoue H. Cationic porphyrins bearing diazolium rings: synthesis and their interaction with calf thymus DNA. Biochim Biophys Acta 1999;1472(1-2):333–43.
[17] Kachadourian R, Batinic-Haberle I, Fridovich I. Synthesis and superoxide dismuting activities of partially (1–4) b-chlorinated derivatives of manganese(III) *meso*-tetrakis(*N*-ethylpyridinium-2-yl)porphyrin. Inorg Chem 1999;38:391–6.
[18] McCord JM, Fridovich I. Superoxide dismutase. An enzymic function for erythrocuprein (hemocuprein). J Biol Chem 1969;244(22):6049–55.
[19] Del Rio LA, Ortega MG, Lopez AL, Gorge JL. A more sensitive modification of the catalase assay with the Clark oxygen electrode. Application to the kinetic study of the pea leaf enzyme. Anal Biochem 1977;80(2):409–15.
[20] Beers RF, Sizer IW. A spectrophotometric method for measuring the breakdown of hydrogen peroxide by catalase. J Biol Chem 1952;195:133–40.
[21] Braughler JM, Pregenzer JF, Chase RL, Duncan LA, Jacobsen EJ, McCall JM. Novel 21-amino steroids as potent inhibitors of iron-dependent lipid peroxidation. J Biol Chem 1987;262(22):10438–40.
[22] Bernheim F, Bernheim MLC, Wilber KM. The reaction between thiobarbituric acid and the oxidation products of certain lipids. J Biol Chem 1948;174:257–64.
[23] Morrow JD, Harris TM, Roberts II LJ. Noncyclooxygenase oxidative formation of a series of novel prostaglandins: analytical ramifications for measurement of eicosanoids. Anal Biochem 1990;184(1):1–10.
[24] Bloodsworth A, O'Donnell VB, Batinic-Haberle I, Chumley PH, Hurt JB, Day BJ, Crow JP, Freeman BA. Manganese-porphyrin reactions with lipids and lipoproteins. Free Radic Biol Med 2000;28(7):1017–29.
[25] Thibodeau PA, Kachadourian R, Lemay R, Bisson M, Day BJ, Paquette B. *In vitro* pro- and antioxidant properties of estrogens. J Steroid Biochem Mol Biol 2002;81(3):227–36.
[26] O'Donnell BV, Tew DG, Jones OT, England PJ. Studies on the inhibitory mechanism of iodonium compounds with special reference to neutrophil NADPH oxidase. Biochem J 1993;290(Pt 1):41–9.

[27] Spasojevic I, Batinic-Haberle I, Reboucas JS, Idemori YM, Fridovich I. Electrostatic contribution in the catalysis of $O_2^{\cdot}$-dismutation by superoxide dismutase mimics. MnIIITE-2-PyP5$^+$ versus MnIIIBr8T-2-PyP$^+$. J Biol Chem 2003;278(9):6831–7.

[28] Sheng H, Enghild JJ, Bowler R, Patel M, Batinic-Haberle I, Calvi CL, Day BJ, Pearlstein RD, Crapo JD, Warner DS. Effects of metalloporphyrin catalytic antioxidants in experimental brain ischemia. Free Radic Biol Med 2002;33(7):947–61.

[29] Holderman MT, Miller KP, Dangott LJ, Ramos KS. Identification of albumin precursor protein, Phi AP3, and alpha-smooth muscle actin as novel components of redox sensing machinery in vascular smooth muscle cells. Mol Pharmacol 2002;61(5):1174–83.

[30] Lennon AM, Ramauge M, Pierre M. Role of redox status on the activation of mitogen-activated protein kinase cascades by NSAIDs. Biochem Pharmacol 2002;63(2):163–70.

[31] Haddad JJ. The involvement of L-gamma-glutamyl-L-cysteinyl-glycine (glutathione/GSH) in the mechanism of redox signaling mediating MAPK(p38)-dependent regulation of pro-inflammatory cytokine production. Biochem Pharmacol 2002;63(2):305–20.

[32] Kamata H, Hirata H. Redox regulation of cellular signalling. Cell Signal 1999;11(1):1–14.

[33] Baker K, Marcus CB, Huffman K, Kruk H, Malfroy B, Doctrow SR. Synthetic combined superoxide dismutase/catalase mimetics are protective as a delayed treatment in a rat stroke model: a key role for reactive oxygen species in ischemic brain injury. J Pharmacol Exp Ther 1998;284(1):215–21.

[34] Milano J, Day BJ. A catalytic antioxidant metalloporphyrin blocks hydrogen peroxide-induced mitochondrial DNA damage. Nucleic Acids Res 2000;28(4):968–73.

[35] Choudhary S, Keshavarzian A, Yong S, Wade M, Bocckino S, Day BJ, Banan A. Novel antioxidants zolimid and AEOL11201 ameliorate colitis in rats. Dig Dis Sci 2001;46(10):2222–30.

[36] Hoffman SW, Moore S, Ellis EF. Isoprostanes: free radical-generated prostaglandins with constrictor effects on cerebral arterioles. Stroke 1997;28(4):844–9.

[37] Lahaie I, Hardy P, Hou X, Hassessian H, Asselin P, Lachapelle P, Almazan G, Varma DR, Morrow JD, Roberts Jr LJ, Chemtob S. A novel mechanism for vasoconstrictor action of 8-isoprostaglandin F2 alpha on retinal vessels. Am J Physiol 1998;274(5 Pt 2): R1406–16.

[38] Massey V. Activation of molecular oxygen by flavins and flavoproteins. J Biol Chem 1994;269(36):22459–62.

[39] Day BJ, Patel M, Calavetta L, Chang LY, Stamler JS. A mechanism of paraquat toxicity involving nitric oxide synthase. Proc Natl Acad Sci USA 1999;96(22):12760–5.

[40] Ganey PE, Kauffman FC, Thurman RG. Oxygen-dependent hepatotoxicity due to doxorubicin: role of reducing equivalent supply in perfused rat liver. Mol Pharmacol 1988;34(5):695–701.

[41] Kagan VE, Tyurina YY. Recycling and redox cycling of phenolic antioxidants. Ann NY Acad Sci 1998;854:425–34.

[42] Pfeiffer S, Schrammel A, Koesling D, Schmidt K, Mayer B. Molecular actions of a Mn(III)Porphyrin superoxide dismutase mimetic and peroxynitrite scavenger: reaction with nitric oxide and direct inhibition of NO synthase and soluble guanylyl cyclase. Mol Pharmacol 1998;53(4):795–800.

[43] Misko TP, Highkin MK, Veenhuizen AW, Manning PT, Stern MK, Currie MG, Salvemini D. Characterization of the cytoprotective action of peroxynitrite decomposition catalysts. J Biol Chem 1998;273(25): 15646–53.

[44] Salvemini D, Riley DP, Lennon PJ, Wang ZQ, Currie MG, Macarthur H, Misko TP. Protective effects of a superoxide dismutase mimetic and peroxynitrite decomposition catalysts in endotoxin-induced intestinal damage. Br J Pharmacol 1999;127(3):685–92.

[45] Cross AH, San M, Stern MK, Keeling RM, Salvemini D, Misko TP. A catalyst of peroxynitrite decomposition inhibits murine experimental autoimmune encephalomyelitis. J Neuroimmunol 2000;107(1):21–8.

[46] Cuzzocrea S, Misko TP, Costantino G, Mazzon E, Micali A, Caputi AP, Macarthur H, Macarthur H, Salvemini D. Beneficial effects of peroxynitrite decomposition catalyst in a rat model of splanchnic artery occlusion and reperfusion. FASEB J 2000;14(9):1061–72.

[47] Naidu BV, Farivar AS, Woolley SM, Fraga C, Salzman AL, Szabo C, Groves JT, Mulligan MS. Enhanced peroxynitrite decomposition protects against experimental obliterative bronchiolitis. Exp Mol Pathol 2003;75(1):12–7.

[48] Pacher P, Liaudet L, Bai P, Mabley JG, Kaminski PM, Virag L, Deb A, Szabo E, Ungvari Z, Wolin MS, Groves JT, Szabo C. Potent metalloporphyrin peroxynitrite decomposition catalyst protects against the development of doxorubicin-induced cardiac dysfunction. Circulation 2003;107(6):896–904.

[49] Szabo C, Mabley JG, Moeller SM, Shimanovich R, Pacher P, Virag L, Soriano FG, Van Duzer JH, Williams W, Salzman AL, Groves JT. Part I: Pathogenetic role of peroxynitrite in the development of diabetes and diabetic vascular complications: studies with FP15, a novel potent peroxynitrite decomposition catalyst. Mol Med 2002;8(10):571–80.